Rare earth element geochemistry of Lake Baikal sediment: Its implication for geochemical response to climate change during the Last Glacial/Interglacial Transition

Kazuya Tanaka[1,*], Fuminori Akagawa[2], Koshi Yamamoto[2], Yukinori Tani[3], Iwao Kawabe[2] and Takayoshi Kawai[2]

[1] Department of Earth and Planetary Systems Science
Graduate School of Science, Hiroshima University
Kagamiyama 1-3-1, Higashi-Hiroshima 739-8526, Japan
[2] Department of Earth and Planetary Science
Graduate School of Environmental Studies, Nagoya University
Chikusa, Nagoya 464-8602, Japan
[3] Institute for Environmental Sciences
University of Shizuoka
52-1 Yada, Shizuoka 422-8526, Japan

Revised version
February 2, 2007

* Corresponding Author: Kazuya Tanaka
e-mail address: tanaka@geol.sci.hiroshima-u.ac.jp
Phone +81-82-424-7459
Fax +81-82-424-0735

Abstract

Sediments deposited on the bottom of Lake Baikal have contributed to the understanding of a long-term environmental history of continents. Rare earth elements (REEs) along with major elements and loss on ignition (LOI) of Baikal sediments were determined with the aim of evaluating their suitability for a new paleoenvironmental proxy. Our interest is concentrated on paleoenvironmental change during the Last Glacial/Interglacial Transition (LGIT). Chondrite-normalized REE patterns for Baikal sediments show a similar variation to those for typical upper continental crustal materials. Three parameters of $(La/Yb)_n$ (n: chondrite-normalized value) ratio, $\sum REE/TiO_2$ and Eu anomaly were used to express detailed characteristics of Baikal sediments. Depth profile of $(La/Yb)_n$ ratio shows abrupt change, whose timing corresponds to the beginning of climatic warming inferred from the profiles of SiO_2/TiO_2 and LOI. In addition, $(La/Yb)_n$ ratio, $\sum REE/TiO_2$ and the degree of Eu anomaly correlate with each other. This suggests that inflow process of particulate materials into the lake may have changed during the Last Glacial/Interglacial Transition. The analytical results of this study lead to the conclusion that REE are a useful paleoenvironmental proxy in the Baikal region.

1. Introduction

Lake Baikal is located in the south of eastern Siberia, close to the Mongolian border. It is 640 km long and 40-50 km wide (widest point 80 km), and the deepest lake on the earth. The average depth of the lake is about 730 m and the maximum 1640 m. Its watershed occupies about 557,000 km^2. The lake itself contains about 23,000 km^3 of water, which is about 20% of the world's reserve of surface fresh water (Van Malderen et al., 1996). This freshwater lake is underlain by a thick sediment sequence (~ 7500 m), which records a continuous history of continental environments (Hutchinson et al., 1992).

Major constituents of Baikal sediment are roughly divided into biogenic and non-biogenic materials. Biogenic components of Baikal sediment are primarily biogenic silica and organic materials. Biological activity is closely related to climatic conditions, and biogenic silica and organic carbon contents of sediments in interglacial periods are higher than those in glacial periods. Diatomaceous ooze and mud are deposited during interglacial periods, whereas diatom-barren silty clay during cold glacial intervals (Prokopenko et al., 1999; Prokopenko et al., 2001a, b). In particular, biogenic silica produced by diatoms has been utilized as a sensitive warm/cold indicator (e.g. Colman et al., 1995; Williams et al., 1997; Prokopenko et al., 2001a, b). On the other hand, non-biogenic materials are mainly detrital silicate minerals, which were transported into the lake via rivers and the air, although authigenic Fe-Mn oxides are observed in some sediment layers (Granina et al., 2004). Since such detrital materials have distinct chemical compositions reflecting their provenance, it is expected that geochemical response to paleoenvironmental change is also recorded in detrital component of sediment. Therefore, studies on chemical composition of Baikal sediment have been advanced (Phedorin et al., 1998; Goldberg et al., 2000; Phedorin et al., 2000a; Phedorin et al., 2000b; Goldberg et al., 2001; Chebykin et al., 2002).

Rare earth elements (REEs) have received considerable attention and contributed to geochemical studies in various fields. This is due to their chemical properties characterized by 4f electronic configurations (Henderson, 1984). In particular, REEs in trivalent state behave as a coherent group of elements in geochemical processes. Cerium and Eu exceptionally change their oxidation states into tetra- and di-valence, respectively, according to redox conditions, which cause their unique and anomalous behavior compared with other REEs. REE abundances in geochemical samples are often discussed using traditional chondrite-normalized patterns plotted against the atomic number, "Masuda-Coryell plot" (Henderson, 1984). The REE abundance patterns provide fingerprints of geochemical processes to form the respective samples. In case of marine environments, REE abundances in Pacific sediments provide the information on the relative contribution of detrital materials (Chinese loess) and authigenic components (Fe-Mn oxides and phosphates: Takebe, 2005). This indicates that REE abundances in sediments have potential of a proxy for earth surface environments. The purpose of this study is to examine whether REE can be a new paleoenvironmental proxy in the Baikal region. For this aim, we focus our interest on the Last Glacial/Interglacial Transition (LGIT).

2. Sample

In this study, we used a 4.66 m core, Ver99-G-12, recovered from Buguldeika Saddle in the Selenga Delta area of Lake Baikal (Fig. 1). The sampling point (52˚31'36"N, 106˚9'8"E) of the core is located near the BDP93 coring site (BDP-93 Baikal Drilling Project Members, 1997). The drill site is characterized by undisturbed hemipelagic sedimentation controlled mainly by the supply of fine suspended particles from the Selenga River, which supplies half of water flowing into Lake Baikal. Radiocarbon (^{14}C) ages of total organic carbon (TOC) in selected Ver99-G-12 core samples were determined by Soma et al. (2006). From the results of their radiocarbon analysis, the average sedimentation rate at the sampling point of Ver99-G-12 was estimated to be about 17.3 cm/1000 yr, which is very close to 17.6 cm/1000 yr at the BDP93 drill site (Colman et al., 1996; Prokopenko et al., 1999). Moreover, the depositional age of the sediment at the bottom of the core was estimated at 27,800 ^{14}C yr B.P., which means that the Ver99-G-12 core covers LGIT.

Forty-seven samples were subsampled for REE and major element analyses at 10 cm intervals from bottom to top of the core except the two samples of the uppermost part subsampled at a 7 cm interval because of lack of a 3 cm thick sediment layer. Additional 12 samples were also subsampled at core depths of 160 – 190 cm and 250 – 280 cm. According to the ^{14}C ages, these two intervals correspond to the Younger Dryas event and LGIT. Each sediment sample was ground with an agate mortar after drying overnight at moderate temperature of about 40˚C.

3. Methods

3.1. REE

REE concentrations in sediment samples were determined by ICP-MS according to the procedures of Yamamoto et al. (2005). About 40 mg of each sample was first digested with 1 ml 38%-HF and 0.5 ml 70%-$HClO_4$ in an open-top Teflon beaker on a hotplate at about 160˚C. After evaporation to dryness, a 0.5 ml mixture of 38%-HF and 70%-$HClO_4$ (2:1 by volume) was added to the residue and again heated at about 160˚C. After complete evaporation of the acids, the residue was dissolved in 2 ml 1.7 M-HCl and centrifuged at 12,000 rpm. The separated residue was fused with about 50 mg of Na_2CO_3-H_3BO_3 (3:1 by weight) in a Pt crucible at 880˚C. The fusion product was dissolved in 1.7 M-HCl and subsequently combined with the 1.7 M-HCl soluble fraction after HF-$HClO_4$ decomposition. Then, REEs in the sample solution were separated from major elements and Ba using cation column exchange chemistry. Finally, each sample solution was adjusted to about 20 ml of 2%-HNO_3 and measured by ICP-MS (HP-4500) at Nagoya University. Details on the analytical procedures and measurement condition in ICP-MS determination are described in Yamamoto et al. (2005).

In order to check analytical accuracy and precision of REE data, we made replicate analyses of a reference rock (JB-1a) issued by the Geological Survey of Japan (GSJ). Results of the replicate analyses are tabulated in Table 1 together with those of Baikal sediment samples. Analytical precision for REE was estimated to be 5% or less. The averages of the replicate analyses are in good agreement with the reference values within errors.

3.2. Major element

Major element concentrations in sediment samples were determined by X-ray fluorescence (XRF) techniques on fused glass beads (Takebe and Yamamoto, 2003). Dry sediment samples were calcined at 1000˚C for 2 hours before preparing glass beads, and then loss on ignition (LOI) was obtained gravimetrically. Glass bead samples were prepared by fusing 0.7 g of the calcined samples with 6.0 g lithium tetraborate in a Pt crucible at 1050˚C. Calibration curves were obtained according to the method of Sugisaki et al. (1977), with GSJ standard rock samples. XRF measurement was performed with a Shimadzu SXF-1200 equipped with a Rh X-ray tube (40 kV, 70 mA) at Nagoya University. Analytical precision for major elements was estimated to be < 1%. The analytical results of major elements and LOI are listed in Table 2.

4. Results

4.1. Profiles of SiO_2/TiO_2 and LOI

The main sources of Si in Baikal sediment are biogenic silica and detrital silicate minerals, while Ti is mainly of detrital origin. Consequently, SiO_2/TiO_2 can be an indicator of the relative contribution of biogenic debris to detrital silicate minerals (e.g. Takebe and Yamamoto, 2003). On the other hand, LOI is practically the sum of organic materials, hydroxyl group of clay minerals and water in biogenic opal (diatom frustules). LOI is also controlled by the relative abundances of biogenic debris (diatom and organic materials) and detrital materials (clay minerals). Oxidation of Fe(II)O to $Fe(III)_2O_3$ during calcination affects LOI values, but it is negligible in the following discussion.

Depth profiles of SiO_2/TiO_2 and LOI for the Ver99-G-12 core samples are shown in Figures 2a and b, respectively. Biogenic silica and TOC reported by Soma et al. (2006) are also plotted for comparison. The contribution of biogenic silica and TOC to SiO_2/TiO_2 and LOI is clearly observed. Both SiO_2/TiO_2 and LOI show an increase at around 280 cm core depth toward the surface of the core, except a drop at around 170 cm core depth. Drops in SiO_2/TiO_2 (biogenic silica) and LOI (TOC) at around 170 cm core depth correspond to the Younger Dryas event. In this way, the Ver99-G-12 core preserves paleoclimatic records during the LGIT.

4.2. REE characteristics of Baikal sediment

Chondrite-normalized REE patterns for Baikal sediments are shown in Figure 3a. The REE patterns exhibit variation typical of the average compositions of upper continental crust such as North American Shale composite (NASC), Post-Archean Australian average shale (PAAS) and Chinese loess (Gromet et al., 1984; Taylor and McLennan, 1988; Gallet et al., 1996). REE patterns for the average shales and Chinese loess are characterized by light REE enrichment and negative Eu anomaly (Fig. 3b). The REE characteristics of the Baikal sediments have no pronounced difference throughout the core samples in the chondrite-normalized patterns (Fig. 3a). Their REE characteristics, however, include small but significant variation as discussed below.

Ratio of La to Yb is often used to express a slope of REE pattern. The $(La/Yb)_n$ ratio (n: chondrite-normalized value) of the Baikal sediments drops sharply at 280 cm core depth (Fig. 4). Except for several samples, the $(La/Yb)_n$ ratios are 9 – 12 above 280 cm core depth, while 11.5 – 14 below 280 cm core depth. The depth of the $(La/Yb)_n$ boundary (i.e. 260 – 280 cm) is consistent with the beginning of climatic warming observed in the depth profiles of SiO_2/TiO_2 and LOI (Figs. 2a and b), although clear response to the Younger Dryas event is not recognized.

5. Discussion

5.1. What controls REE characteristics?

We use here two parameters of Total REE (∑REE) /TiO_2 and Eu anomaly as well as $(La/Yb)_n$ in order to discuss the REE characteristics of Baikal sediments in more detail. ∑REE is normalized to TiO_2 because REE concentrations of bulk sediment samples are diluted by biogenic silica with low REE contents. These three parameters show good correlations with each other (Figs. 5a, b and c).

In order to assess the potential of REE as a paleoenvironmental proxy, we should consider what controls REE abundances of sediment. As mentioned above, Baikal sediments consist of biogenic materials (diatom frustules and organic materials) and non-biogenic materials (detrital materials and authigenic Fe-Mn oxide). Biogenic silica does not contribute to bulk REE amounts of sediments and solely dilutes bulk REE concentrations. It is well-known that Fe-Mn oxide, such as deep sea ferromanganese nodules, is highly enriched in REE (e. g. Elderfield et al., 1981; Ohta et al., 1999). However, the contribution of Fe-Mn oxides is possibly minor because Fe and Mn concentrations do not correlate with $\sum REE/TiO_2$, Eu anomaly and $(La/Yb)_n$ (Figs. 6a and b). It is also unlikely that organic materials control these REE characteristics because of low TOC of 0.5 – 3.6% (Soma et al., 2006). Probably, inorganic detrital materials predominantly control REE characteristics of Baikal sediment in the Selenga area.

5.2. Response of detrital component to climatic change

From Figure 4 and the correlation observed in Figures 5a, b and c, two hypotheses on the change of paleoenvironment surrounding Lake Baikal can be conducted: One is the possibility that inflow process of particulate materials into the lake via the Selenga River may have changed during the LGIT. Change of the Selenga River system, which covers a huge catchment area, could result in transportation of different particle composition. For example, abundance of heavy minerals in sediment, even if it is minor, can affect bulk REE concentrations because they are highly enriched in REE (Gromet and Silver, 1983; Suzuki et al., 1990). The other is the possibility that the relative contribution of aeolian dust to riverine particulate materials may have changed. This is linked to flux of aeolian dust and riverine particles into Lake Baikal. Bobrov et al. (2001) analyzed REE concentrations in aeolian and riverine suspended particles in the Selenga area. Their data show that $(La/Yb)_n$ ratio of aeolian dust is 7.6, whereas those of riverine particles are 12.5 – 13.8. This suggests that REE abundances in Baikal sediment may be explained by mixing of aeolian and riverine particles. If the second possibility is accepted, the relative flux of aeolian dust in the post glacial period is higher than that in the last glacial period. However, the second possibility is inconsistent with previous works, which suggested the importance of the contribution of aeolian dust during arid glacial periods (Peck et al., 1994; Edgington et al., 1996). Therefore, the first possibility is more acceptable than the second one.

It has been demonstrated that REE characteristics in Baikal sediments preserve paleoenvironmental records during the LGIT (Figs. 4, 5a, b and c). It is expected that the use of REE is extended to long core samples in order to discuss long-term glacial/interglacial cycles.

6. Conclusions

We analyzed major elements, LOI and REEs in Baikal sediments of a short core in the Selenga Delta area. The potential of REE as a new paleoenvironmental proxy were examined in this study. Depth profiles of SiO_2/TiO_2 and LOI exhibit variation reflecting climatic change during the LGIT. This means that the core used in this study preserves good climatic records and is suitable for the examination of REE. Chondrite-normalized REE patterns for Baikal sediments are very similar to those for typical upper continental crustal materials. Depth profile of $(La/Yb)_n$ ratio shows abrupt change at the middle of the core. The timing of the change corresponds to the beginning of climatic warming inferred from the profiles of SiO_2/TiO_2 and LOI. Furthermore, three parameters of $(La/Yb)_n$ ratio, $\sum REE/TiO_2$ and Eu anomaly correlate with each other. This suggests that the Selenga River system may have changed during the LGIT. From our analytical results, it can be concluded that REEs are a useful indicator to trace the circulation of detrital materials in the Baikal region.

Acknowledgements

This work was supported by a grant from the Ministry of Education, Culture, Sports, Science and Technology, Japan (Dynamics of the Sun-Earth-Life Interactive System, No.G-4, the 21st Century

COE Program). Constructive reviews by Prof. J. Rose and an anonymous reviewer improved the earlier manuscript.

References

Anders, E., Grevesse, N., 1989. Abundances of the elements: Meteoritic and solar. Geochimica et Cosmochimica Acta 53, 197-214.

BDP Baikal Drilling Project Members, 1997. Preliminary results of the first scientific drilling on Lake Baikal, Buguldeika site, southeastern Siberia. Quaternary International 37, 3-17.

Bobrov, V. A., Granina, L. Z., Kolmogorov, Yu. P., Melgunov, M. S., 2001. Minor elements in aeorian and riverine suspended particles in Baikal region. Nuclear Instruments and Methods in Physics Research A 470, 431-436.

Chebykin, E. P., Edgington, D. N., Grachev, M. A., Zheleznyakova, T. O., Vorobyova, S. S., Kulikova, N. S., Azarova, I. N., Khlystov, O. M., Goldberg, E. L., 2002. Abrupt increase in precipitation and weathering of soils in East Siberia coincident with the end of the last glaciation (15 cal kyr BP). Earth and Planetary Science Letters. 200, 167-175.

Colman, S. M., Peck, J. A., Karabanov, E. B., Carter, S. J., Bradbury, J. P., King, J.W., Williams, D. F., 1995. Continental climate response to orbital forcing from biogenic silica records in Lake Baikal. Nature 378, 769-771.

Colman, S. M., Jones, G. A., Rubin, M., King, J. W., Peck, J. A., Orem, W. H., 1996. AMS radiocarbon analyses from Lake Baikal, Siberia: Challenges of dating sediments from a large, oligotrophic lake. Quaternary Science Reviews (Quaternary Geochronology) 15, 669-684.

Edgington, D. N., Robbins, J. A., Colman, S. M., Orlandini, K. A., Gustin, M. -P., 1996. Uranium-series disequilibrium, sedimentation, diatom frustules, and paleoclimate change in Lake Baikal. Earth and Planetary Science Letters 142, 29-42.

Elderfield, E., Hawkensworth, C. J., Greaves, M. J., Calvert, S. E., 1981. Rare earth element geochemistry of oceanic ferromanganese nodules and associated sediments. Geochimica et Cosmochimica Acta 45, 513-528.

Gallet, S., Jahn, B.-m., Torii, M., 1996. Geochemical characterization of the Luochuan loess-paleosol sequence, China, and paleoclimatic implications. Chemical Geology 133, 67-88.

Goldberg, E. L., Phedorin, M. A., Grachev, M. A., Bobrov, V. A., Dolbnya, I. P., Khlystov, O. M., Levina, O. V., Ziborova, G. A., 2000. Geochemical signals of orbital forcing in the records of paleoclimates found in the sediments of Lake Baikal. Nuclear Instruments and Methods in Physics Research A 448, 384-393.

Goldberg, E. L., Grachev, M. A., Phedorin, M. A., Kalugin, I. A., Khlystov, O. M., Mezentsev, S. N., Azarova, I. N., Vorobyeva, S. S., Zheleznyakova, T. O., Kulipanov, G. N., Kondratyev, V. I., Miginsky, E. G., Tsukanov, V. M., Zolotarev, K. V., Trunova, V. A., Kolmogorov, Yu. P., Bobrov, V. A., 2001. Application of synchrotron X-ray fluorescent analysis to studies of the records of paleoclimates of Eurasia stored in the sediments of Lake Baikal and Lake Teletskoye. Nuclear Instruments and Methods in Physics Research A 470, 388-395.

Granina, L., Müller, B., Wehrli, B., 2004. Origin and dynamics of Fe and Mn sedimentary layers in Lake Baikal. Chemical Geology 205, 55-72.

Gromet, L. P., Silver, L. T., 1983. Rare earth element distributions among minerals in a granodiorite and their petrogenetic implications. Geochimica et Cosmochimica Acta 47, 925-939.

Gromet, L. P., Dymek, R. F., Haskin, L. A., Korotev, R. L., 1984. The "North American shale composite": its compilation, major and trace element characteristics. Geochimica et Cosmochimica Acta 48, 2469-3482.

Henderson, P., 1984. General geochemical properties and abundances of the rare earth elements. In: Henderson, P. (Ed.), Rare Earth Element Geochemistry. Elsevier, New York, pp. 1-32.

Hutchinson, D. R., Golmshtok, A. J., Zonenshain, L. P., Moore, T. C., Scholz, C. A., Kitgord, K. D., 1992. Depositional and tectonic framework of the rift basins of Lake Baikal from multichannel seismic data. Geology 20, 589-592.

Kawabe, I., Toriumi, T. Ohta, A., Miura, N., 1998. Monoisotopic REE abundances in seawater and the origin of seawater tetrad effect. Geochemical Journal 32, 213-229.

Ohta, A., Ishii, S., Sakakibara, M., Mizuno, A., Kawabe, I., 1999. Systematic correlation of the Ce anomaly with the Co/(Ni + Cu) ratio and Y fractionation from Ho in distinct types of Pacific deep-sea nodules. Geochemical Journal 33, 399-417.

Peck, J. A., King, J. W., Colman, S. M., Kravchinsky, V. A., 1994. A rock magnetic record from Lake Baikal, Siberia: evidence for Late Quaternary climate change. Earth and Planetary Science Letters 122, 221-238.

Phedorin, M. A., Bobrov, V. A., Zolotarev, K. V., 1998. Synchrotron radiation X-ray fluorescence analysis on VEPP-3 of the bottom sediments of Lake Baikal to perform a paleoclimatic reconstruction. Nuclear Instruments and Methods in Physics Research A 405, 560-568.

Phedorin, M. A., Bobrov, V. A., Goldberg, E. L., Navez, J., Zolotaryov, K. V., Grachev, M. A., 2000a. SR-XFA as a method of choice in the search of signals of changing palaeoclimates in the sediments of Lake Baikal, compared to INAA and ICP-MS. Nuclear Instruments and Methods in Physics Research A 448, 394-399.

Phedorin, M. A., Goldberg, E. L., Grachev, M. A., Levina, O. L., Khlystov, O. M., Dolbnya, I. P., 2000b. The comparison of biogenic silica, Br and Nd distributions in the sediments of Lake Baikal as proxies of changing paleoclimates of the last 480 kyr. Nuclear Instruments and Methods in Physics Research A 448, 400-406.

Prokopenko, A. A., Williams, D. F., Karabanov, E. B., Khursevich, G. K., 1999. Response of Lake Baikal ecosystem to climate forcing and pCO_2 change over the last/interglacial transition. Earth and Planetary Science Letters 172, 239-253.

Prokopenko, A. A., Karabanov, E. B., Williams, D. F., Kuzmin, M. I., Shackleton, N. J., Crowhurst, S. J., Peck, J. A., Gvozdkov, A. N., King, J. W., 2001a. Biogenic silica record of the Lake Baikal response to climatic forcing during the Brunhes. Quaternary Research 55, 123-132.

Prokopenko, A. A., Karabanov, E. B., Williams, D. F., Kuzmin, M. I., Khursevich, G. K., Gvozdkov, A. A., 2001b. The detailed record of climatic events during the past 75,000 yrs BP from the Lake Baikal drill core BDP-93-2. Quaternary International 80-81, 59-68.

Soma, Y., Tani, Y., Soma, M., Mitake, H., Kurihara, R., Hashomoto, S., Watanabe, T., Nakamura, T., 2006. Sedimentary steryl chlorin esters (SCEs) and other photosynthetic pigments as indicators of paleolimnological change over the last 28,000 years from the Buguldeika Saddle of Lake Baikal. Journal of Paleolimnology DOI 10.1007/s10933-006-9011-z.

Sugisaki, R., Shimomura, T., Ando, K., 1977. An automatic X-ray fluorescence method for the analysis of silicate rocks. Journal of Geological Society of Japan 83, 725-733.

Suzuki, K., Adachi, M., Yamamoto, K., 1990. Possible effects of grain-boundary REE on the REE distribution in felsic melts derived by partial melting. Geochemical Journal 24, 57-74.

Takebe, M., 2005. Carriers of rare earth elements in Pacific deep-sea sediments. The Journal of Geology 113, 201-215.

Takebe, M., Yamamoto, K., 2003. Geochemical fractionation between porcellanite and host sediment. The Journal of Geology 111, 301-312.

Taylor, S. R., McLennan, S. M., 1988. The significance of the rare earths in geochemistry and cosmochemistry. In: Gschneidner Jr. K. A., Eyring, L. (Eds.), Handbook on the Physics and Chemistry of Rare Earths. Elsevier, Amsterdam, vol. 11, pp. 485-578.

Van Malderen, H., Van Grieken, R., Khodzher, T., Obolkin, V., Potemkin, V., 1996. Composition of individual aerosol particles above Lake Baikal, Siberia. Atmospheric Environment 30, 1453-1465.

Williams, D. F., Peck, J., Karabanov, E. B., Prokopenko, A. A., Kravchinsky, V., King, J., Kuzmin, M. I., 1997. Lake Baikal record of continental climate response to orbital insolation during the past 5 million years. Science 278, 1114-1117.

Yamamoto, K., Yamashita, F., Adachi, M., 2005. Precise determination of REE for sedimentary rocks issued by the Geological Survey of Japan. Geochemical Journal 39, 289-297.

Figure captions

Figure 1. Location map showing core sampling site of Ver99-G-12.

Figure 2. Depth profiles of (a) SiO_2/TiO_2 and (b) LOI. Biogenic silica and TOC data by Soma et al. (2006) are also plotted for comparison. The age-depth model is based on Soma et al. (2006).

Figure 3. (a) Chondrite-normalized REE patterns for Baikal sediments. (b) Comparison of REE patterns between the average of Baikal sediment and typical upper continental materials. Chondritic values by Anders and Grevesse (1989) are used for normalization with a modification of Tb (0.0348 ppm), Ho (0.0525 ppm) and Tm (0.0234 ppm) (Ebihara, M., personal communication, 2002). REE data of PAAS and Chinese loess are quoted from Taylor and McLennan (1988) and Gallet et al. (1996), respectively. NASC values of Gromet et al. (1984) modified by Kawabe et al. (1998) are also plotted.

Figure 4. Depth profile of $(La/Yb)_n$ ratio, where the suffix "n" denotes a chondrite-normalized value. The age-depth model is based on Soma et al. (2006).

Figure 5. Correlation plots between $\sum REE/TiO_2$, Eu anomaly and $(La/Yb)_n$. $\sum REE$ is recalculated on LOI free basis. Europium anomaly is defined as $\log\{Eu_n/(Sm_n \times Gd_n)\}$. The data above 280 cm are plotted as a dotted circle, while those below 280 cm as a filled circle.

Figure 6. $\sum REE/TiO_2$ plotted against (a) Fe_2O_3/TiO_2 and (b) MnO/TiO_2.

Table 1. Analytical results of REE concentrations in Baikal sediment and JB-1a.

Sample No	depth (cm)	La (ppm)	Ce (ppm)	Pr (ppm)	Nd (ppm)	Sm (ppm)	Eu (ppm)	Gd (ppm)	Tb (ppm)	Dy (ppm)	Ho (ppm)	Er (ppm)	Tm (ppm)	Yb (ppm)	Lu (ppm)	Total REE (ppm)
1	460	68.0	136	15.7	59.4	10.3	1.81	8.39	1.17	7.09	1.40	4.03	0.563	3.82	0.548	318
2	450	51.6	101	11.5	44.0	7.89	1.53	6.83	0.974	6.01	1.19	3.53	0.499	3.34	0.476	240
3	440	45.4	90.0	10.5	40.3	7.27	1.44	6.25	0.904	5.59	1.13	3.24	0.456	3.11	0.448	216
4	430	63.7	126	14.2	53.6	9.28	1.72	7.82	1.11	6.82	1.37	3.87	0.544	3.68	0.523	295
5	420	73.8	148	17.0	64.5	11.0	1.90	9.03	1.28	7.80	1.55	4.39	0.612	4.21	0.601	345
6	410	66.5	133	15.1	57.2	9.81	1.70	7.98	1.13	6.89	1.37	3.87	0.533	3.60	0.501	309
7	400	71.4	146	16.5	62.1	10.7	1.77	8.60	1.20	7.34	1.45	4.10	0.574	3.92	0.547	336
8	390	66.1	136	14.6	54.6	9.32	1.70	7.73	1.07	6.51	1.28	3.59	0.491	3.33	0.468	307
9	380	56.4	113	12.4	47.0	8.16	1.54	6.68	0.931	5.65	1.13	3.16	0.434	2.98	0.416	260
10	370	75.3	156	16.2	60.5	10.2	1.79	8.52	1.18	7.18	1.42	3.96	0.551	3.75	0.515	347
11	360	73.4	153	16.0	60.2	10.3	1.80	8.52	1.21	7.24	1.44	4.04	0.564	3.80	0.533	342
12	350	73.3	153	16.3	60.6	10.3	1.71	8.51	1.19	7.28	1.44	4.16	0.585	3.96	0.565	343
13	340	50.5	101	11.1	42.5	7.53	1.48	6.38	0.903	5.49	1.08	3.14	0.434	2.96	0.423	235
14	330	74.0	152	16.4	61.5	10.5	1.81	8.54	1.19	7.21	1.41	4.05	0.567	3.85	0.548	344
15	320	61.0	122	13.5	50.9	8.82	1.59	7.25	1.03	6.29	1.24	3.59	0.501	3.41	0.490	282
16	310	62.1	125	13.6	51.3	8.79	1.62	7.33	1.03	6.27	1.23	3.57	0.499	3.39	0.481	287
17	300	56.0	112	12.3	46.8	8.21	1.55	6.86	0.961	5.88	1.15	3.32	0.459	3.15	0.451	259
18	290	54.4	109	12.0	45.6	8.03	1.53	6.83	0.962	5.93	1.16	3.38	0.466	3.22	0.455	253
19	280	73.0	144	15.9	59.5	10.2	1.77	8.38	1.18	7.13	1.40	4.04	0.567	3.81	0.546	332
4-3-1	275.6	57.7	119	12.7	48.0	8.49	1.59	6.89	1.01	6.18	1.21	3.55	0.506	3.37	0.495	271
4-2-1	273.4	49.1	99.5	11.0	42.0	7.52	1.48	6.33	0.912	5.59	1.10	3.24	0.465	3.11	0.453	232
20	270	51.8	104	11.6	44.3	7.96	1.51	6.76	0.964	6.04	1.19	3.48	0.481	3.31	0.465	244
3-43-1	266.6	47.3	95.6	10.7	41.3	7.52	1.48	6.42	0.941	5.84	1.17	3.45	0.496	3.33	0.489	226
3-42-1	264.3	58.2	118	12.9	48.7	8.54	1.60	6.99	1.02	6.23	1.23	3.63	0.519	3.49	0.509	272
21	260	48.6	96.1	10.7	40.8	7.21	1.41	6.18	0.869	5.40	1.07	3.06	0.433	2.97	0.422	225
3-39-1	257.5	48.9	96.6	10.8	41.4	7.32	1.41	6.09	0.887	5.46	1.07	3.21	0.455	3.10	0.454	227
3-38-1	255.2	50.8	99.9	11.3	43.3	7.71	1.49	6.53	0.939	5.70	1.12	3.30	0.467	3.14	0.458	236
22	250	45.6	89.8	10.4	39.9	7.28	1.41	6.27	0.912	5.73	1.12	3.38	0.471	3.25	0.467	216
23	240	48.9	95.9	11.0	41.7	7.62	1.48	6.67	0.937	5.90	1.14	3.52	0.492	3.45	0.489	229
24	230	44.2	87.8	10.2	39.6	7.34	1.44	6.42	0.889	5.66	1.09	3.27	0.459	3.19	0.447	212
25	220	40.0	79.6	9.36	36.4	6.65	1.35	5.93	0.795	5.08	0.980	2.91	0.401	2.84	0.403	193
26	210	46.5	92.7	10.7	41.3	7.41	1.40	6.23	0.872	5.46	1.07	3.11	0.430	3.00	0.423	221
27	200	41.9	81.1	9.49	37.3	6.77	1.34	5.93	0.830	5.17	1.02	2.98	0.407	2.82	0.405	197
28	190	44.1	87.7	10.3	40.4	7.53	1.49	6.76	0.976	6.14	1.22	3.56	0.495	3.40	0.482	214
3-8-1	187.1	39.7	79.9	9.27	36.4	6.79	1.37	6.01	0.897	5.61	1.12	3.36	0.476	3.24	0.474	195
3-7-1	184.8	46.6	92.4	10.7	41.9	7.74	1.52	6.83	1.00	6.30	1.25	3.71	0.525	3.50	0.515	224
29	180	48.0	91.9	10.9	42.5	7.70	1.53	6.78	0.944	5.85	1.15	3.36	0.455	3.19	0.457	225
3-3-1	175.7	44.1	86.1	10.2	39.6	7.34	1.46	6.36	0.919	5.65	1.12	3.32	0.472	3.17	0.474	210
3-2-1	173.4	44.7	86.6	10.2	40.1	7.40	1.47	6.45	0.946	5.88	1.17	3.46	0.487	3.32	0.491	213
30	170	47.2	95.6	10.6	41.0	7.45	1.49	6.51	0.927	5.74	1.13	3.29	0.456	3.12	0.448	225
2-43-1	166.6	56.3	108	12.7	48.5	8.62	1.62	7.21	1.04	6.23	1.23	3.61	0.507	3.38	0.502	259
2-42-1	164.3	52.2	101	11.8	45.3	8.14	1.58	6.91	0.985	5.99	1.18	3.49	0.496	3.31	0.492	242
31	160	54.6	105	12.2	47.0	8.52	1.61	7.49	1.05	6.54	1.29	3.81	0.523	3.58	0.518	254
32	150	51.2	101	11.8	45.4	8.27	1.60	7.18	0.999	6.12	1.17	3.59	0.492	3.39	0.486	242
33	140	40.7	80.4	9.64	38.1	6.88	1.36	5.64	0.767	4.62	0.890	2.59	0.361	2.51	0.358	195
34	130	44.3	83.7	10.3	40.5	7.35	1.47	6.33	0.873	5.37	1.05	3.06	0.431	2.97	0.432	208
35	120	47.8	89.0	10.7	42.1	7.53	1.49	6.39	0.883	5.37	1.04	2.99	0.413	2.84	0.407	219
36	110	42.8	80.2	9.77	38.0	6.85	1.36	5.96	0.810	4.89	0.952	2.67	0.371	2.56	0.362	197
37	100	51.6	97.1	11.4	43.9	7.76	1.46	6.64	0.924	5.50	1.09	3.11	0.429	2.95	0.424	234
38	90	47.5	85.3	10.5	40.3	7.21	1.42	6.26	0.854	5.16	1.02	2.88	0.399	2.75	0.397	212
39	80	36.8	71.0	8.82	34.4	6.28	1.26	5.35	0.729	4.41	0.863	2.51	0.343	2.48	0.352	176
40	70	33.8	63.6	7.98	31.3	5.66	1.13	4.68	0.638	3.89	0.764	2.19	0.309	2.19	0.306	158
41	60	48.4	85.2	10.5	40.6	7.24	1.42	6.37	0.870	5.24	1.03	2.90	0.392	2.73	0.386	213
42	50	43.0	78.8	9.82	38.3	6.94	1.37	6.04	0.826	4.93	0.979	2.76	0.384	2.65	0.385	197
43	40	40.4	74.7	9.26	36.2	6.57	1.29	5.63	0.776	4.69	0.915	2.64	0.363	2.55	0.364	186
44	30	49.8	84.9	9.86	36.6	6.06	1.13	5.14	0.695	4.16	0.811	2.33	0.317	2.25	0.318	204
45	20	34.5	63.8	7.93	30.8	5.51	1.04	4.71	0.639	3.85	0.753	2.13	0.286	2.04	0.278	158
46	10	30.6	56.8	7.06	27.6	4.93	0.937	4.27	0.574	3.51	0.685	1.92	0.262	1.87	0.262	141
47	3	31.8	59.7	7.39	28.6	5.19	0.977	4.47	0.620	3.75	0.743	2.09	0.286	2.04	0.287	148
JB-1a																
average	(n = 12)	35.7	62.9	6.70	25.7	4.80	1.38	4.52	0.648	3.96	0.763	2.20	0.300	2.00	0.283	
S.D.	(n = 12)	0.5	0.9	0.1	0.4	0.08	0.02	0.05	0.012	0.05	0.011	0.05	0.008	0.03	0.007	
reference*		37.6	65.9	7.30	26.0	5.07	1.46	4.67	0.690	3.99	0.71	2.18	0.330	2.1	0.330	
S.D.		2.5	5.0	1.87	3.1	0.38	0.078	0.53	0.072	0.68	0.140	0.47	0.065	0.21	0.046	

* Data of the reference values of JB-1a are quoted from the web site of the Geological Survey of Japan (http://www.aist.go.jp/RIODB/db012/welcome.html).

Table 2. Major element analyses of Baikal sediment after calcination at 1000℃.

Sample No.	depth (cm)	Fe_2O_3 (%)	CaO (%)	K_2O (%)	TiO_2 (%)	MnO (%)	MgO (%)	SiO_2 (%)	Na_2O (%)	Al_2O_3 (%)	P_2O_5 (%)	Total (%)	LOI (%)
1	460	8.69	3.07	2.73	1.01	0.096	3.01	61.3	2.16	16.9	0.200	99.2	6.86
2	450	7.94	2.05	3.12	0.935	0.122	3.09	62.2	1.75	17.0	0.169	98.4	7.47
3	440	8.73	1.75	3.09	0.949	0.085	3.19	61.8	1.73	17.5	0.180	99.0	7.79
4	430	8.70	2.62	2.92	0.971	0.140	2.83	61.5	2.03	17.4	0.194	99.3	6.65
5	420	8.48	3.30	2.72	1.02	0.095	2.80	60.9	2.21	16.2	0.189	97.9	6.25
6	410	8.67	2.52	3.14	0.944	0.097	2.97	61.2	2.14	18.0	0.201	100.0	7.44
7	400	10.1	2.05	3.13	0.980	0.083	2.49	59.4	1.78	17.3	0.170	97.4	8.50
8	390	8.63	2.14	3.10	0.995	0.128	3.07	61.5	1.90	18.1	0.186	99.8	7.55
9	380	8.23	2.24	3.15	0.949	0.142	2.83	61.7	1.97	17.9	0.191	99.2	6.76
10	370	8.10	2.52	3.05	0.989	0.106	2.83	61.8	1.97	17.6	0.186	99.1	6.62
11	360	7.97	2.60	3.11	0.964	0.119	2.94	61.5	2.13	17.7	0.198	99.3	6.97
12	350	9.17	2.47	3.20	0.947	0.201	2.74	60.7	1.97	17.3	0.190	98.8	6.65
13	340	8.08	2.50	3.06	0.971	0.108	3.19	60.2	2.06	18.4	0.187	98.7	6.93
14	330	8.46	2.55	3.18	0.965	0.108	2.95	61.8	2.14	18.1	0.184	100.4	7.08
15	320	8.49	2.22	3.24	0.951	0.113	2.82	59.8	1.84	18.2	0.187	97.8	6.97
16	310	7.90	2.47	3.22	0.983	0.096	3.02	61.1	2.02	17.8	0.176	98.8	6.69
17	300	8.30	2.25	3.32	0.974	0.100	3.21	60.3	2.10	18.8	0.187	99.5	6.97
18	290	8.51	2.36	3.25	0.989	0.131	3.16	59.8	2.00	18.2	0.200	98.6	6.81
19	280	8.30	2.26	3.26	0.949	0.163	2.94	60.6	2.15	18.0	0.187	98.8	6.84
4-3-1	275.6	8.47	2.36	3.21	0.956	0.123	2.93	59.8	2.00	17.7	0.191	97.7	5.94
4-2-1	273.4	8.08	2.04	3.44	0.954	0.115	3.06	60.8	1.89	18.2	0.187	98.8	6.16
20	270	8.08	2.20	3.09	0.951	0.156	3.11	61.7	1.79	17.1	0.177	98.4	7.66
3-43-1	266.6	7.87	1.99	3.04	1.02	0.126	3.04	61.7	1.68	17.3	0.222	98.0	6.32
3-42-1	264.3	7.79	2.57	2.94	0.976	0.102	2.96	61.4	1.96	17.1	0.177	98.0	6.44
21	260	7.68	2.30	3.07	0.883	0.089	2.95	62.2	2.15	17.4	0.176	98.8	7.21
3-39-1	257.5	8.02	2.28	2.98	0.915	0.129	2.84	61.2	1.94	17.2	0.217	97.7	6.18
3-38-1	255.2	8.28	2.15	3.07	0.938	0.174	2.95	60.8	1.90	17.4	0.249	97.9	6.24
22	250	7.51	2.77	3.06	0.914	0.091	3.72	61.8	1.82	17.3	0.168	99.1	8.40
23	240	8.75	2.27	2.87	0.913	0.104	3.01	62.4	2.05	16.8	0.209	99.4	7.63
24	230	8.51	2.00	2.99	0.930	0.092	3.01	61.8	1.81	16.8	0.162	98.1	8.27
25	220	7.51	2.01	2.80	0.811	0.096	2.54	64.4	2.08	16.2	0.190	98.7	8.74
26	210	8.19	1.96	2.87	0.828	0.084	2.67	65.0	2.03	16.3	0.198	100.1	8.98
27	200	7.51	1.77	2.67	0.791	0.092	2.59	65.9	1.70	15.0	0.167	98.3	9.31
28	190	7.16	2.00	2.95	0.932	0.120	3.37	64.9	1.67	16.9	0.156	100.2	9.77
3-8-1	187.1	6.77	2.76	2.85	0.922	0.089	3.81	62.6	1.37	16.1	0.150	97.3	9.67
3-7-1	184.8	7.30	2.29	2.89	0.902	0.092	3.25	62.6	1.54	16.4	0.163	97.4	8.40
29	180	7.89	1.86	2.95	0.900	0.068	3.09	63.5	1.83	16.8	0.173	99.1	8.92
3-3-1	175.7	10.0	1.83	2.84	0.916	0.090	2.92	61.1	1.51	16.1	0.173	97.5	8.57
3-2-1	173.4	7.90	1.89	2.93	0.912	0.101	2.96	62.8	1.57	16.8	0.179	98.0	7.82
30	170	8.59	1.95	3.18	0.937	0.187	3.13	61.2	1.85	18.0	0.190	99.2	7.50
2-43-1	166.6	8.73	2.13	2.92	0.927	0.100	2.62	61.8	1.89	17.0	0.205	98.4	8.64
2-42-1	164.3	8.33	2.19	2.88	0.949	0.105	2.62	61.7	1.98	16.8	0.215	97.7	8.61
31	160	9.29	2.32	2.89	0.873	0.092	2.76	61.7	2.04	16.6	0.205	98.7	10.0
32	150	9.55	2.26	3.09	0.906	0.101	2.90	60.6	2.26	17.5	0.253	99.4	10.5
33	140	9.69	2.03	2.98	0.885	0.099	2.71	59.4	2.11	16.8	0.255	97.0	10.6
34	130	9.04	2.15	2.82	0.897	0.099	2.80	62.8	2.17	17.1	0.240	100.0	11.5
35	120	7.89	2.17	2.73	0.824	0.099	2.64	63.9	2.09	16.1	0.228	98.7	10.9
36	110	7.72	2.07	2.47	0.776	0.094	2.31	66.2	1.83	14.5	0.208	98.2	11.0
37	100	7.79	2.38	2.51	0.812	0.109	2.51	65.4	1.93	15.2	0.197	98.8	11.8
38	90	7.40	2.15	2.49	0.783	0.101	2.46	67.2	2.00	15.2	0.199	100.0	12.1
39	80	8.37	1.96	2.40	0.752	0.080	2.28	66.1	1.97	14.6	0.223	98.7	12.5
40	70	7.04	1.81	2.20	0.693	0.072	2.06	69.6	1.71	13.3	0.202	98.7	12.5
41	60	7.15	2.01	2.35	0.737	0.075	2.32	67.3	1.85	14.6	0.204	98.6	12.7
42	50	7.17	2.28	2.40	0.763	0.092	2.42	67.9	1.98	14.7	0.221	100.0	12.1
43	40	6.33	2.09	2.27	0.704	0.096	2.24	69.3	1.87	13.9	0.206	99.1	11.6
44	30	7.38	1.95	1.97	0.631	0.173	2.01	71.0	1.45	12.1	0.445	99.1	11.8
45	20	6.51	1.69	1.90	0.573	0.178	1.83	73.0	1.41	11.7	0.665	99.4	11.4
46	10	5.81	1.61	1.73	0.540	0.131	1.75	76.9	1.30	10.8	0.303	100.9	11.4
47	3	6.95	1.52	1.81	0.582	0.120	1.82	73.9	1.37	11.5	0.320	99.9	11.6

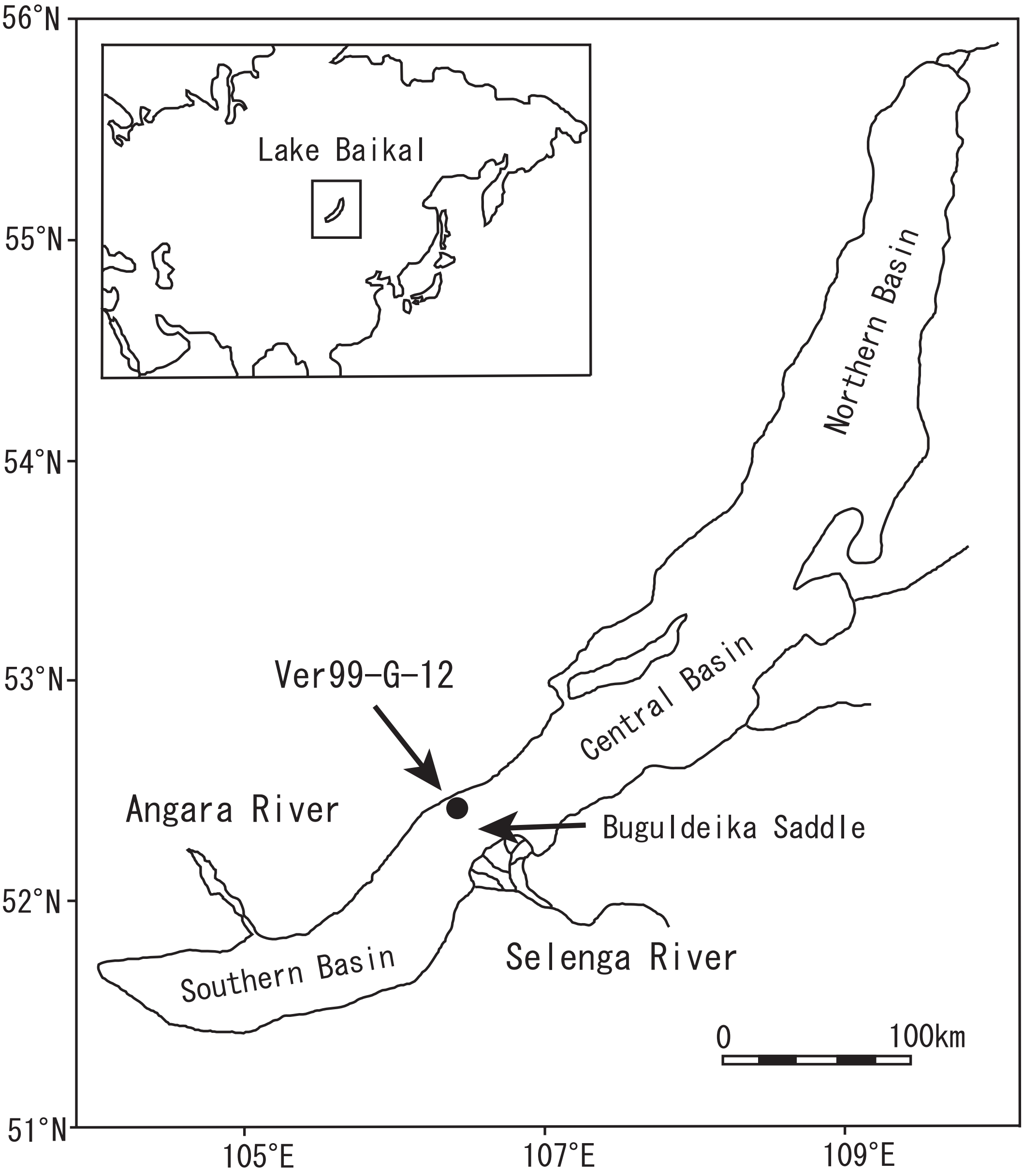

Fig. 1 Tanaka et al.

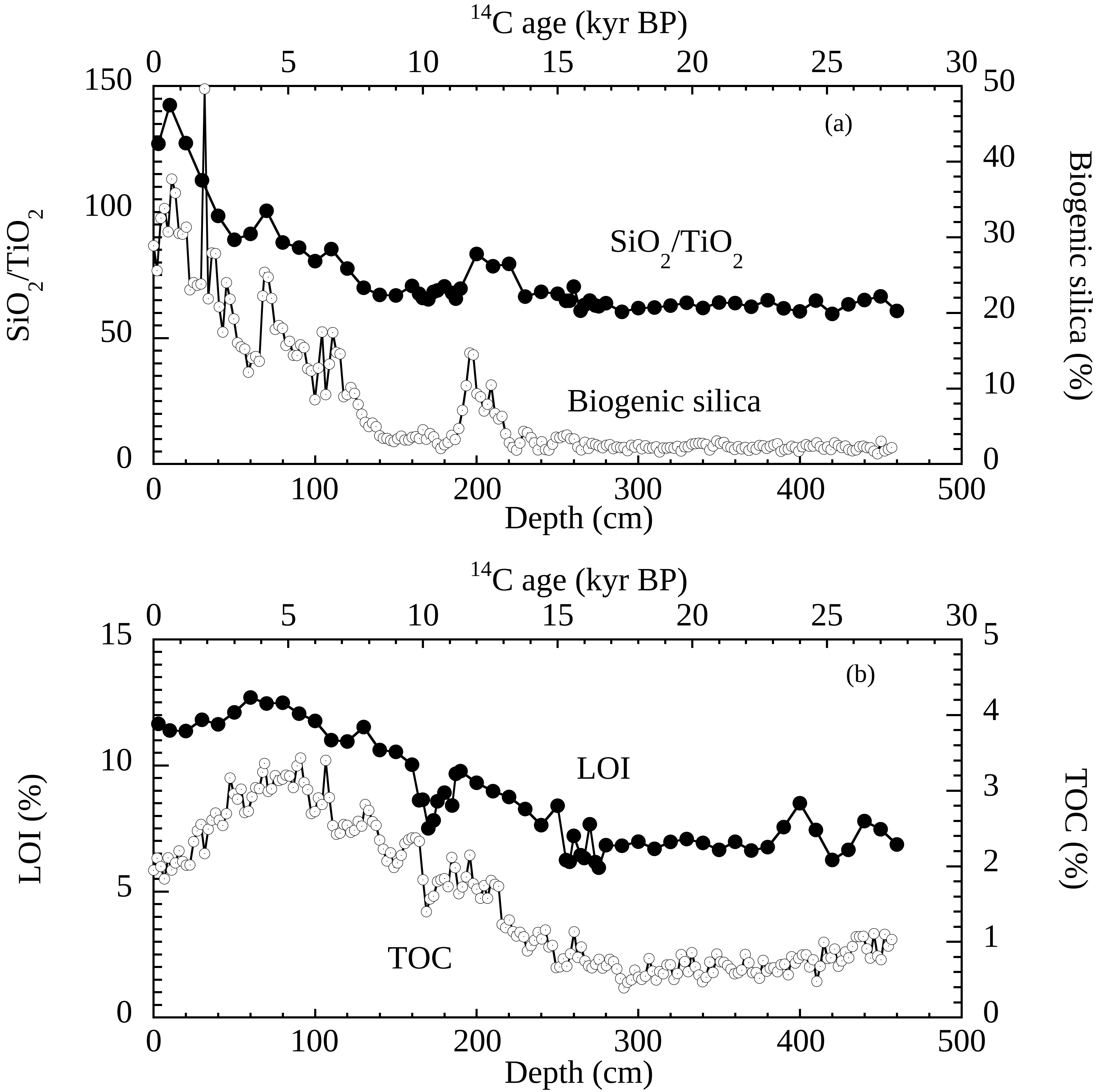

Fig. 2. Tanaka et al.

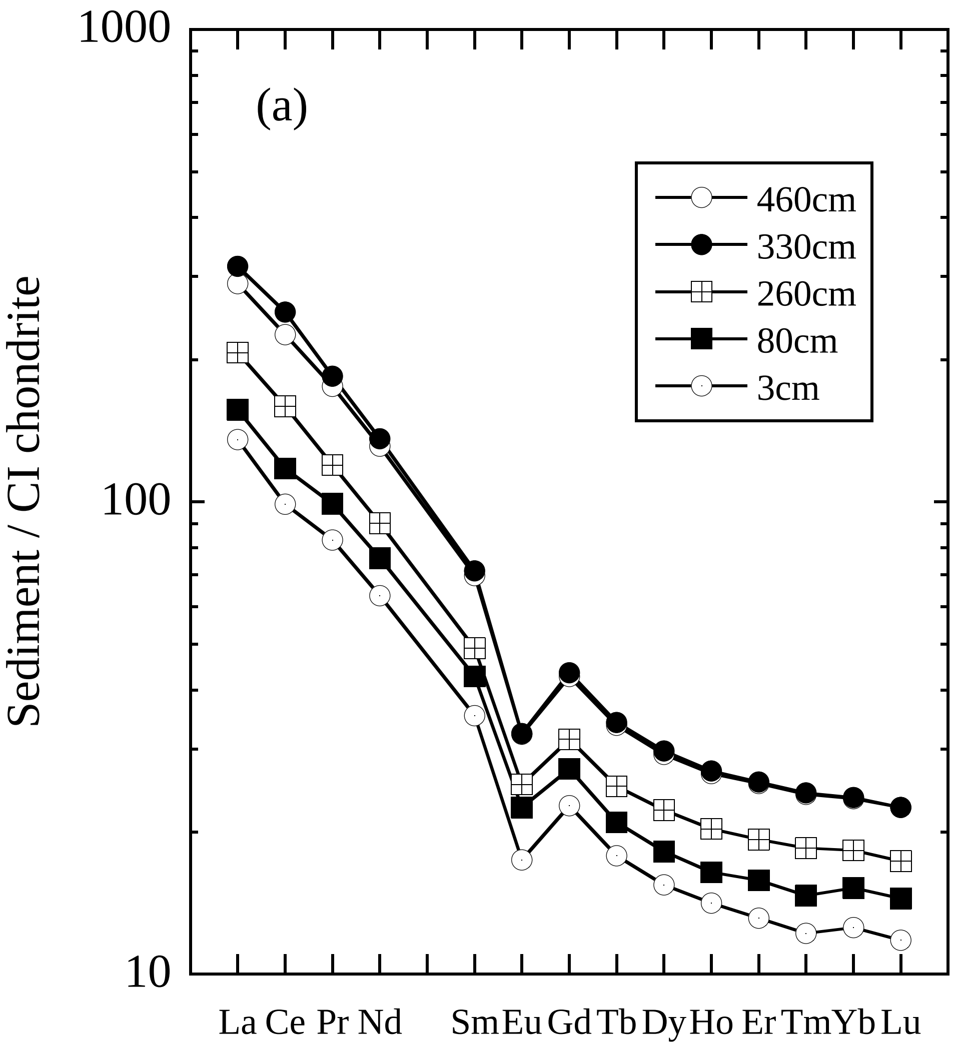

Fig. 3a Tanaka et al.

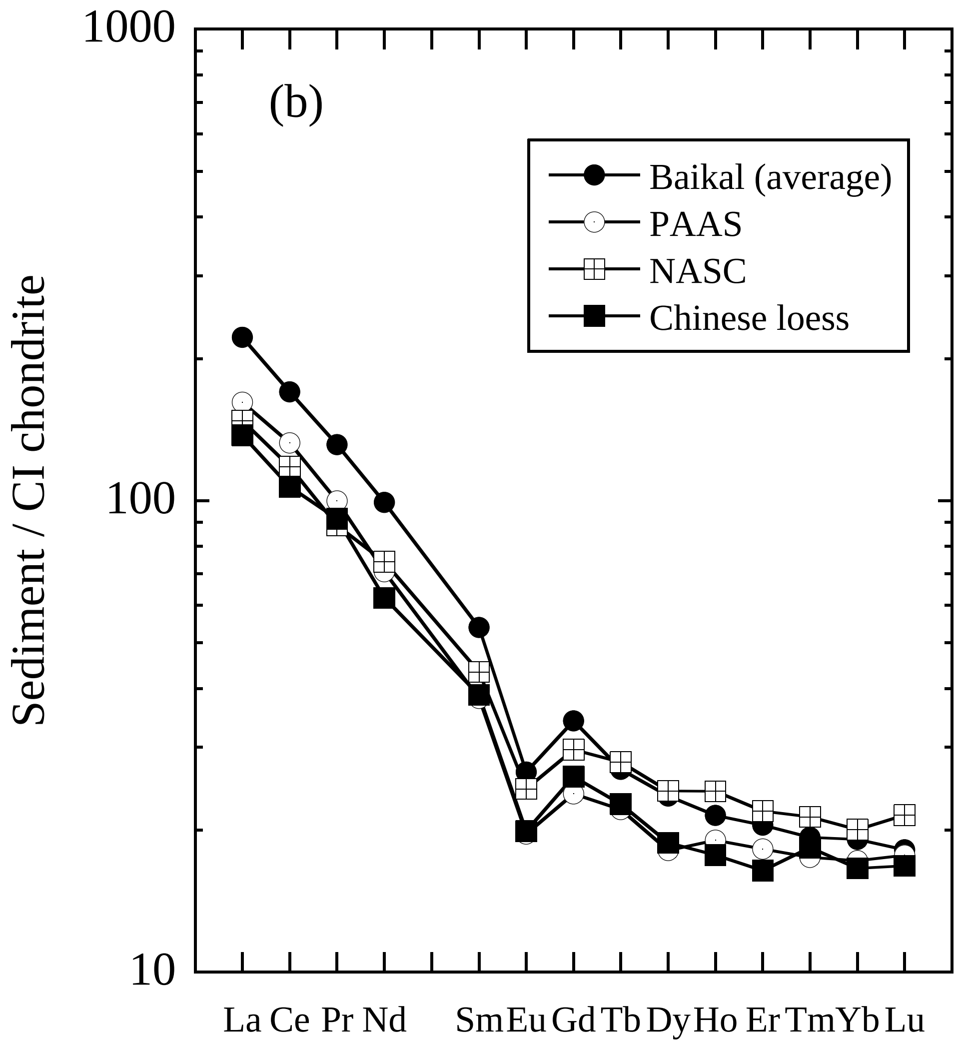

Fig. 3b Tanaka et al.

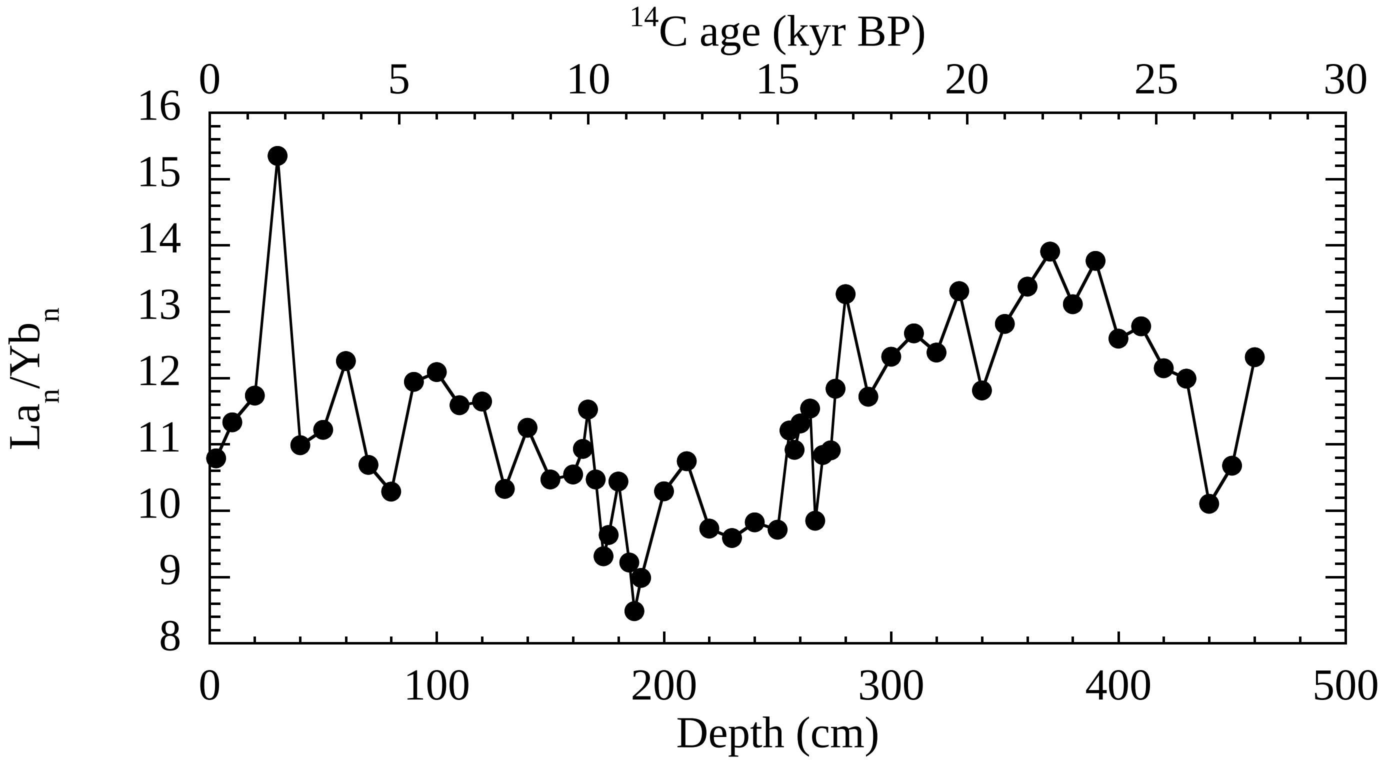

Fig. 4. Tanaka et al.

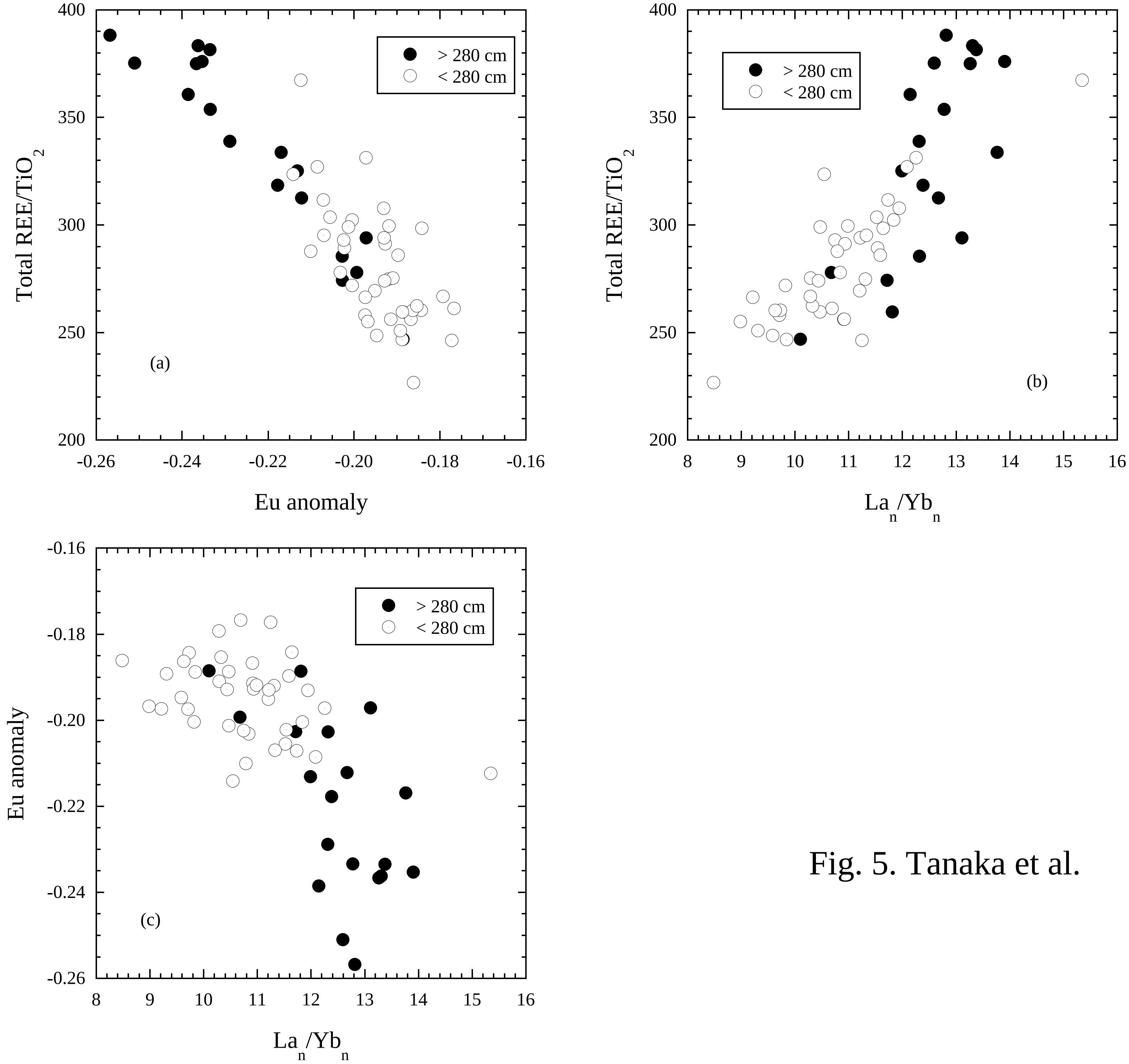

Fig. 5. Tanaka et al.

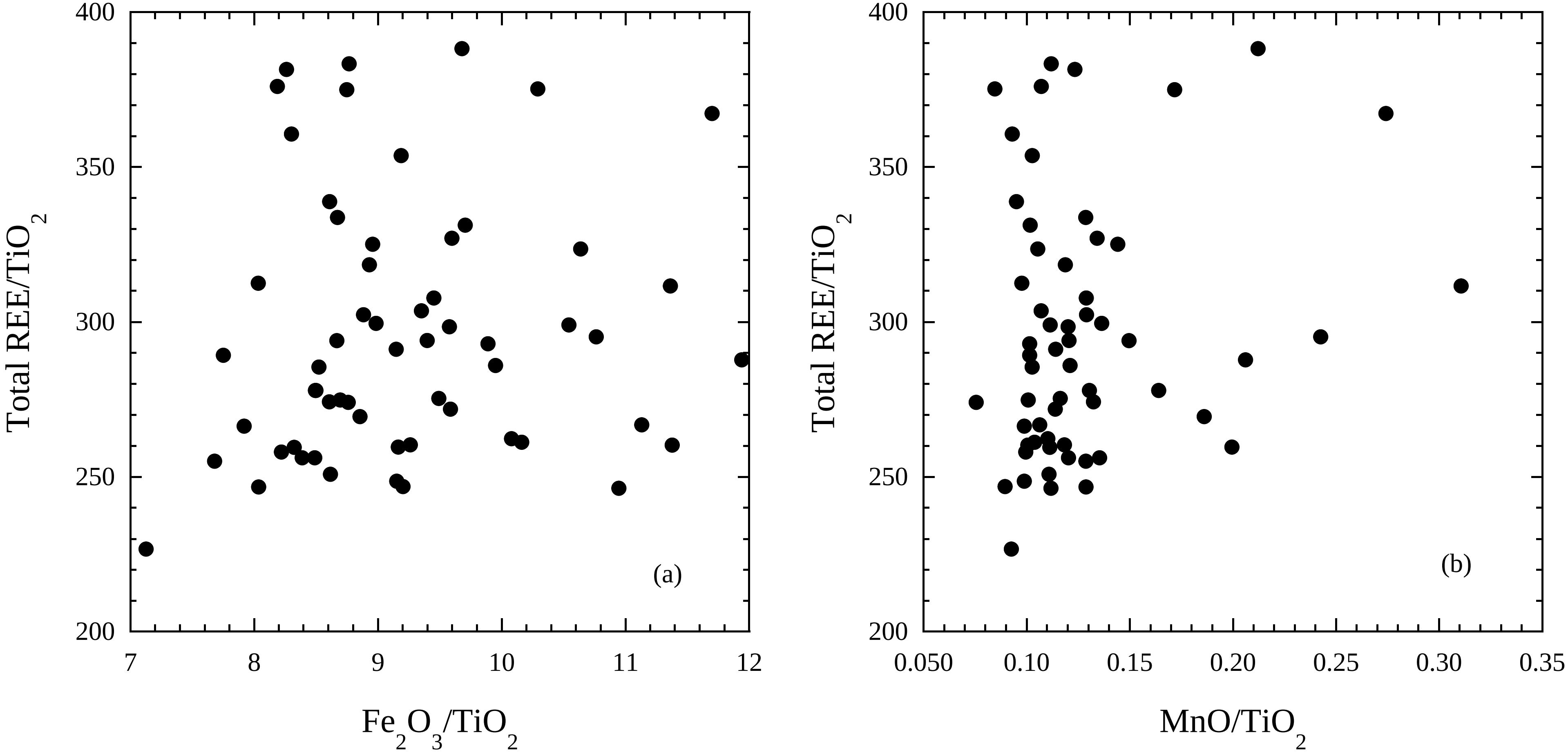

Fig. 6. Tanaka et al.